

Subduction on the northern and southern flanks of the Gulf Stream

LEIF N. THOMAS *

DEPARTMENT OF ENVIRONMENTAL EARTH SYSTEM SCIENCE

STANFORD UNIVERSITY

STANFORD, CALIFORNIA

TERRENCE M. JOYCE

DEPARTMENT OF PHYSICAL OCEANOGRAPHY

WOODS HOLE OCEANOGRAPHIC INSTITUTION

WOODS HOLE, MASSACHUSETTS

* *Corresponding author address:* Leif N. Thomas, Dept. of Environmental Earth System Science, Stanford University, Stanford, CA 94305-4020.

E-mail: leift@stanford.edu

ABSTRACT

Sections of temperature, salinity, dissolved oxygen, and velocity were made crossing the Gulf Stream in late January 2006 to investigate the role of frontal processes in the formation of Eighteen Degree Water (EDW), the Subtropical Mode Water of the North Atlantic. The sections were nominally perpendicular to the Stream and measured in a Lagrangian frame by following a floating spar buoy drifting in the Gulf Stream's warm core. During the survey, EDW was isolated from the mixed layer by the stratified seasonal pycnocline, suggesting that EDW was not yet actively being formed at this time in the season and at the longitudes over which the survey was conducted (64 to 70 W). However, on two of the sections, the seasonal pycnocline in the core of the Gulf Stream was broken by an intrusion of cold, fresh, weakly-stratified water nearly saturated in oxygen that appears to have been subducted from the surface mixed layer north of the Stream. The intrusion was identified on three of the sections in profiles with a nearly identical temperature-salinity relation. From the western- to easternmost sections where the intrusion was observed, the depth of the intrusion's salinity minimum descended by ~ 90 m in the 71 hours it took to complete this part of the survey. This apparent subduction occurred primarily on the upstream side of a meander trough where the cross-stream velocity was confluent and frontogenetic. Using a variant of the omega equation, the vertical velocity driven by the confluent flow was inferred and yielded downwelling in the vicinity of the intrusion spanning from 10-40 m day^{-1} , a range of values consistent with the intrusion's observed descent, suggesting that frontal subduction was responsible

for the formation of the intrusion. On the easternmost section located downstream of the meander trough, the flow was diffluent, driving an inferred vertical circulation that was of the opposite sense as that on the section upstream of the trough. In transiting the two sides of the trough, the intrusion was observed to move towards the center of the Stream between the downwelling branches of the opposing vertical circulations, resulting in a downward Lagrangian mean vertical velocity and net subduction. Hydrographic evidence of subduction of weakly stratified surface waters was seen on the southern flank of the Gulf Stream as well. The solution of the omega equation suggests that this subduction was associated with a relatively shallow vertical circulation confined to the upper 200 m of the water column in the proximity of the front marking the southern edge of the warm core.

1. Introduction

Subduction is the process by which water from the surface mixed layer is transferred into the ocean interior. It is a process that is critical for the transport of dynamical and biogeochemical tracers such as heat, salt, potential vorticity and dissolved gases to the pycnocline from the mixed layer where they are modified by air-sea fluxes. Subduction can be driven by both thermodynamical and mechanical means, such as through shoaling of the mixed layer by buoyancy gain, Ekman pumping, and lateral transfer of water across a sloping mixed layer base (Marshall et al. 1993; Huang and Qiu 1994). In eddy rich regions of the ocean such as near ocean fronts, the combination of outcropping isopycnals and eddy-driven ageostrophic motions is conducive to subduction (Spall 1995; Marshall 1997). In this article, direct evidence of such frontal subduction is presented from observations taken near the Gulf Stream as part of the CLIMODE experiment (e.g. The CLIMODE Group 2008) which seeks to address the role of lateral mixing in the upper ocean on air-sea fluxes and formation of Eighteen Degree Water (EDW, Worthington (1959)), and to assess where EDW forms and where it circulates after formation.

2. Methods and measurements

Fifty-two hydrographic stations were occupied during a cruise aboard the R/V *Atlantis* in the proximity of the Gulf Stream from January 18-31, 2006. The stations were taken along four lines that were nominally oriented perpendicular to the Gulf Stream (figure 1). Along each line the distance between stations was ~ 15 km. The zonal location of each line

was chosen to approximately intersect the trajectory of a floating spar buoy that had been deployed to the south of the Gulf Stream in the region of minimum vertical shear.

At each station a CTD was deployed, yielding either 1000 or 2000 m deep profiles of temperature, salinity, dissolved oxygen and pressure averaged to 2 m resolution. Water samples for oxygen, salinity, nutrients and DIC/Total Alkalinity analyses were also collected, the results of which will not be discussed here. To identify surface waters that had recently been subducted, the apparent oxygen utilization, $\text{AOU} = \acute{O}_2 - O_2$ (\acute{O}_2 is the solubility of oxygen given the temperature and salinity at a particular depth, and O_2 is the measured concentration of oxygen at that depth) was calculated. Surface water is nearly saturated in oxygen and is therefore distinguishable as water with low AOU.

Horizontal velocities were measured continuously using a 75 kHz ADCP that was installed on the Atlantis, yielding velocity profiles with a vertical resolution of 8 m and a vertical extent of up to 800 m.

To facilitate the intercomparison of measurements made on the four lines, the observations were mapped to a common coordinate system whose x -axis was nominally perpendicular to the Gulf Stream. The coordinate system was constructed as follows. On each line, the depth-averaged velocity was calculated and then averaged in latitude bins 0.05° wide yielding velocities (\bar{U}, \bar{V}) . The bin where the depth-averaged speed was maximum, with geographical coordinates (x_o, y_o) , determined the center of the coordinate system on each line. The direction of the velocity vector at (x_o, y_o) , i.e. $\phi = \tan^{-1}(\bar{V}/\bar{U}) \Big|_{(x_o, y_o)}$, set the cross-stream coordinate, i.e. $x_s = (x - x_o) \sin \phi - (y - y_o) \cos \phi$. Velocity measurements from the ADCP, (u, v) , were then projected into along-stream (v_s) and cross-stream (u_s) components: $v_s = u \cos \phi + v \sin \phi$, $u_s = u \sin \phi - v \cos \phi$.

Once the cross-stream coordinate was obtained, vertical sections of hydrography and velocity were constructed from the individual profiles by performing a one dimensional cross-stream objective map at each vertical level. The form of the correlation function used in the mapping was Gaussian with a correlation length of 15 km for temperature, salinity, density, and oxygen and 10 km for velocity.

3. Results

Cross-stream sections of salinity, AOU, down-stream velocity, and potential density are shown in figure 2 for line 3. Features common to all four lines are described below. In the axis of the Gulf Stream the permanent pycnocline ascends towards the surface and down-stream velocities are characterized by a surface-intensified jet with speeds up to 2.2 m s^{-1} . In the top $\sim 150 \text{ m}$, isopycnals with density less than 25.9 kg m^{-3} take a bowl-like shape and mark the boundary of the Gulf Stream’s warm core where water temperatures were observed to be as high as $22 \text{ }^\circ\text{C}$. In the stratified region at the base of the warm core, the value of the salinity can exceed 36.7 psu. Such high salinities are characteristic of the so-called “Salinity Maximum Water” (SMW, Worthington (1976)) which originates in the central tropical Atlantic under the region of high net evaporation. The larger value of AOU in the SMW indicates that SMW is relatively depleted in oxygen and has thus been out of contact with the atmosphere for a longer period of time relative to its surrounding waters. To the south of the Gulf Stream and in the ocean interior, there is a voluminous watermass with low AOU ($20\text{-}30 \text{ } \mu\text{moles kg}^{-1}$), a mean temperature, salinity, and density of $18.3 \text{ }^\circ\text{C}$, 36.6 psu, and 26.4 kg m^{-3} , respectively, and anomalously weak stratification and hence low planetary

potential vorticity (PV) $q_p = fN^2$ (f is the Coriolis parameter, $N^2 = \partial b / \partial z$, $b = -g\rho/\rho_o$ is the buoyancy, g is the acceleration due to gravity, ρ is the density, and ρ_o is a reference density). This corresponds to EDW, the subtropical mode water of the North Atlantic. At this early stage in the winter season, the EDW was capped by the seasonal pycnocline that effectively acts as a high PV barrier shielding the EDW from atmospheric forcing. As a consequence, no isopycnals denser than 26.3 kg m^{-3} outcrop, indicating that EDW was not actively being ventilated at this relatively western portion of the Gulf Stream. However, above the EDW, $\sim 200 \text{ m}$ thick mixed layers were observed with water nearly saturated in oxygen (i.e. $\text{AOU} = 2 - 10 \text{ } \mu\text{moles kg}^{-1}$), suggesting that mixed layer deepening had and was occurring and that later in the season the EDW would be exposed to the atmosphere.

On line 3, at station 31, the high-PV barrier was broken by an anomalously fresh thermohaline intrusion with low PV (Figure 2). The intrusion was not observed at adjacent stations, suggesting that it was less than 30 km wide. There are indications that it was seen at stations 22 and 41, which were taken on lines 2 and 4, respectively (Figure 3). The temperature-salinity relation at stations 22, 31, and 41 are nearly identical, implying that the same water mass had been sampled at the three stations. The intrusion is identified as a prominent cusp in the T-S relation, with a salinity of 34.8 psu and temperature $12.9 \text{ }^\circ\text{C}$ which were anomalously low relative to nearby waters on the 26.3 kg m^{-3} isopycnal on which the intrusion was found. At station 22, the intrusion was in the surface mixed layer at $x_s = -32 \text{ km}$, i.e. to the north of the Gulf Stream. By stations 31 and 41 it had moved closer to the center of the Stream to positions $x_s = -25 \text{ km}$ and $x_s = -14 \text{ km}$, respectively. The intrusion had also descended in the vertical, leaving the surface mixed layer. In the interior, the intrusion formed a pycnostad with anomalously weak stratification, low PV,

and low AOU. These observations suggest that the intrusion was subducted from the surface mixed layer north of the Stream along the downward sloping 26.3 kg m^{-3} isopycnal surface.

The downward displacement of the intrusion was quantified by calculating the lagged correlation between salinity profiles from stations 22, 31, and 41 (see Figure 4). The lag (and hence vertical displacement) where the correlation between salinity profiles from stations 22 and 31 (31 and 41) was maximum was 60 m (30 m). The time in between casts 22 and 31 and 31 and 41 was 31 and 40 hours, respectively. Given the estimated vertical displacements between stations, and assuming that hydrographic measurements were quasi-Lagrangian, that is, nearly the same water parcels had been tracked on all three stations, this would yield vertical velocities of ~ 45 and $\sim 20 \text{ m day}^{-1}$ between the two station pairs.

A comment should be made regarding to what extent the hydrographic measurements were Lagrangian. The striking similarity in water properties observed on casts 22, 31, and 41 in a region of strong lateral thermohaline variability, suggests that nearly the same water parcels had been tracked on the three stations. This tracking of the intrusion was not completely by chance, as the hydrographic sections were made following a floating spar buoy traveling with the Stream. Having said this, it is not obvious that tracking the spar buoy would result in a quasi-Lagrangian measurement near the intrusion since the buoy was located far to its south (e.g. Figure 1). However, the isotach of v_s corresponding to the depth-averaged down-stream velocity at the location of the spar buoy happened to intersect the intrusion where it had been observed on sections 2-4 (see Figure 2) suggesting that both the intrusion and spar buoy were subject to nearly the same down-stream velocity. Consequentially, since the sections were made following the spar buoy, the hydrographic measurements at casts 22, 31, 41 at the depth of the intrusion can be treated as being

quasi-Lagrangian.

The largest descent occurred between lines 2 and 3, on the upstream side of a meander trough (see Figure 1). At greater depths, in the main thermocline of the Gulf Stream, downward vertical motions have similarly been observed on the upstream side of meander trough (Bower and Rossby 1989; Lindstrom et al. 1997). On this side of a trough the frontal jet tends to be confluent and hence frontogenetic. Indeed, the observations of the cross-stream velocity along line 2 reveal a confluent flow with velocities directed towards the center of the Stream on either side of $x_s = 0$ (Figure 5). In contrast, the cross-stream velocity on line 4 was directed away from the center of the Stream (Figure 5). Line 4 crossed the front on the downstream side of meander trough. On this side of a meander, as confirmed by the observations, the flow tends to be diffluent and frontolytic. A frontogenetic (frontolytic) strain field will disrupt the thermal wind balance and drive a thermally direct (indirect) vertical circulation to restore geostrophy in accordance with the omega equation (Hoskins et al. 1978). To determine if the observed strain field was responsible for the apparent subduction of the thermohaline intrusion, the vertical circulation was quantified by solving a variant of the omega equation, as described in the next section.

4. Quantification of the frontal vertical circulation

The flow can be split into geostrophic and ageostrophic components: $u_s = u_g + u_{ag}$, $v_s = v_g + v_{ag}$. Using the traditional assumption often invoked at ocean fronts that cross-front variations are much greater than along-front variations, the cross-stream ageostrophic flow can be written in terms of a scalar streamfunction, ψ , i.e. $u_{ag} = \partial\psi/\partial z$, $w = -\partial\psi/\partial x_s$.

A single equation for the streamfunction can be derived for subinertial ageostrophic motions, which for inviscid, adiabatic, quasi-geostrophic flows is given by

$$f^2 \frac{\partial^2 \psi}{\partial z^2} + N^2 \frac{\partial^2 \psi}{\partial x_s^2} = 2 \left(\frac{\partial u_g}{\partial x_s} \frac{\partial b}{\partial x_s} + \frac{\partial v_g}{\partial x_s} \frac{\partial b}{\partial y_s} \right), \quad (1)$$

(Hoskins et al. 1978; Pollard and Regier 1992). Estimates of the two terms on the right hand side (RHS) of (1) based on the hydrographic, velocity, and satellite SST observations show that the first term dominates the forcing ¹. The lack of resolution in the along-stream direction makes it difficult to estimate the across-stream component of the geostrophic flow u_g . On account of this, the observed cross-stream velocity u_s shown in Figure 5 was used to calculate the first term on the RHS of (1) instead of u_g . The measured cross-stream velocity has both geostrophic and ageostrophic contributions. By using u_s instead of u_g , it is assumed that the ageostrophic velocity is much weaker than the geostrophic flow. This assumption can be checked a priori (at least with the portion of the ageostrophic flow that is governed by (1)) by comparing the magnitude of $\partial \psi / \partial z$ to u_s . Other ageostrophic motions, say due to inertial oscillations, could be present, however it is unlikely that they contribute to the large scale confluent/diffluent pattern in u_s seen in Figure 5. The vertical velocity was inferred by solving (1) using these approximations and subject to a $w = 0$ boundary condition at the edges of the domain in which the calculation was performed, i.e.: $\psi = 0$ at $z = 0, -H$

¹Satellite SST measurements were used to estimate the structure and magnitudes of both terms on the RHS of (1) near the surface. Both terms had a similar cross-front structure indicating that they would drive overturning in the same sense. However, the magnitude of term one was larger than term two, suggesting that it is the dominant forcing term. The implication being that the vertical velocity inferred using term 1 is likely a good measure of w .

($H = 800$ m) and $\partial\psi/\partial x_s = 0$ at $x_s = x_1, x_2$ ($x_1 = -60$ km, $x_2 = 80$ km)². The vertical velocity inferred in this manner is shown in Figure 6.

On line 2, the solution is characterized by two overturning cells: a deep cell centered around $x_s = 0$ with downwelling on the northern wall of the Gulf Stream and a shallow cell centered near station 18, with a downdraft on the southern edge of the warm core. Both vertical circulations are thermally direct, i.e. tending to restratify the fluid, as to be expected since the flow is driven by a frontogenetic strain field. The cross-stream ageostrophic velocity associated with the overturning cells is weaker than the observed u_s (i.e. $\partial\psi/\partial z$ does not exceed 0.08 m s⁻¹), suggesting that u_s on line 2 is primarily ascribable to a geostrophic flow, as had been assumed to solve (1). At the location of the intrusion on lines 2 and 3 (-170 m $< z < -50$ m, -32 km $< x_s < -25$ km, $\rho = 26.3$ kg m⁻³) the inferred vertical velocity is negative and ranges between 10 to 40 m day⁻¹, values that are consistent with the observed descent of the intrusion.

A single overturning cell dominates the inferred vertical velocity field on line 4. As was to be expected given the frontolytic flow field on this line, the vertical circulation is thermally indirect with upwelling and downwelling on the dense and less dense side of the

²Setting $w = 0$ at the bottom of the domain is somewhat of an arbitrary constraint often used in studies of frontal vertical circulation (e.g. Pollard and Regier 1992; Allen and Smeed 1996; Rudnick 1996; Thomas et al. 2009). Therefore, it is critical to push the bottom of the domain as far from the region of interest as possible so that the inferred w is not greatly affected by the boundary condition. In this application, the region of interest is near the thermohaline intrusion ($z \approx -100$ m), which is far from the bottom of the domain at $z = -800$ m. It was found that pushing the bottom boundary down an additional 200 m (setting the right hand side of (1) to zero below -800 m where there is no velocity data) had only a minor effect on w , suggesting that the boundary condition did not greatly affect the solution.

front, respectively. The calculation suggests that the vertical circulation averaged in the along-stream direction is weaker than that on a given section since the thermally direct and indirect circulations on the down and upstream sides of meander troughs would tend to cancel. However this Eulerian mean vertical circulation is not necessarily equal to the average vertical circulation following fluid parcels. The Lagrangian mean vertical velocity is the relevant quantity for assessing net subduction and can differ from the Eulerian mean velocity by a Stokes drift (Andrews et al. 1987). The shift in the cross-stream location of the observed thermohaline intrusion suggests that Lagrangian parcels on the dense side of the front were displaced towards the center of the Stream from line 2 to 4. Moving downstream between these two lines the vertical circulation changes sign, however it appears that the intrusion by being displaced towards the center of the Stream tends to remain in the downwelling branches of both the thermally direct and indirect circulations (i.e. casts 22 and 41 are located in regions where $w < 0$), suggesting that the Lagrangian mean vertical velocity and Stokes drift is downward.

The hydrographic observations of the thermohaline intrusion clearly support the idea that strain associated with meanders drives subduction of surface waters near the northern wall of the GS. The structure of the PV on line 3 suggests that subduction had also occurred on the southern edge of the warm core. As can be seen in Figure 2, low PV water at $z \approx -175$ m near station 28 is associated with a pycnostad that extends to the south and connects surface and interior waters, outcropping in the mixed layer near station 26. A pycnostad with similar watermass properties, oxygen concentration, and density to that near station 28 was seen at station 18 (Figure 7). The solution to the omega equation suggests that station 18 was located in the downwelling branch of the southern, shallow overturning cell,

implying that water sampled at that station should experience a downward displacement as it progresses downstream. Comparing the vertical profiles of the salinity at stations 18 and 28, reveals that the halocline capping the pycnostad does indeed appear to have been displaced downward from line 2 to line 3. A downward displacement of 40 m results from the lagged correlation between the two salinity profiles (Figure 4). If the water sampled in the pycnostad at stations 18 and 28 were identical, then its vertical velocity would be estimated by dividing the downward displacement by the ~ 36 hour time interval between casts. However, unlike casts 22, 31, and 41 which approximately intersected the isotach corresponding to the velocity of the ASIS buoy, and hence were taken in a quasi-Lagrangian frame, casts 18 and 28 are located to the south of this isotach, in a region where the downstream velocity was weaker by a factor of 0.63-0.76. Therefore it is likely that the time it takes fluid parcels to traverse the distance between stations 18 and 28 is more on the order of 50 rather than 36 hours. If we accept this longer timescale and assume the flow field to be stationary in time, then the 40 m vertical displacement inferred from the vertical structure of the two casts would translate to a downward velocity of 19 m day^{-1} , a value similar to the downwelling in the southern overturning cell seen in Figure 6.

In the diagnostic for the vertical velocity used above, it is assumed that the vertical circulation is driven solely by shear and strain in the geostrophic flow field. Other processes such as wind-induced frictional forces, diabatic processes, time-dependent near and super inertial motions, or higher order corrections to the quasi-geostrophic omega equation could also generate vertical motions (Viúdez et al. 1996; Giordani et al. 2006; Nagai et al. 2006; Thomas et al. 2009). For example, a spatially uniform wind blowing over a current with lateral variations in vertical vorticity will generate Ekman pumping/suction owing to the

modification of the Ekman transport by the vorticity (Stern 1965; Niiler 1969). On line 2 this effect was estimated to drive vertical velocities with magnitudes less than 4 m day^{-1} , much smaller than those inferred using the omega equation. The small amplitude of this wind-driven vertical velocity is primarily attributable to the weakness of the wind stress on line 2 (i.e. the magnitude of the average down-stream component of the stress on this line was equal to 0.03 N m^{-2}). Diabatic processes that drive lateral variations in mixing of buoyancy (which for example could be generated by heat loss or the Ekman advection denser water over light that arises when winds blow along a front) will disrupt the thermal wind balance and hence induce an ageostrophic circulation (Thomas et al. 2009). Scalings for this effect suggest that the vertical velocities that it would induce are an order of magnitude smaller than that predicted by the omega equation. These scaling arguments combined with the finding that the vertical velocities inferred from the Lagrangian analysis and the solution to (1) are consistent implies that the bulk of the downward motions responsible for the subduction and formation of the intrusion and pycnostad can be explained by the physics of the quasi-geostrophic omega equation.

5. Conclusions

Wintertime cross-stream hydrographic and velocity sections of the Gulf Stream have revealed direct evidence of the formation via frontal subduction of a thermohaline intrusion and a low PV pycnostad on the northern and southern boundaries of the current, respectively. Vertical velocity estimates based on the omega-equation and the vertical displacement of the intrusion and pycnostad suggest that the strain field associated with Gulf Stream meanders

was responsible for the $\sim 20 - 45 \text{ m day}^{-1}$ downward velocities of the features. This vertical velocity is one to two orders of magnitude larger than the maximum in the annually averaged vertical velocity associated with lateral induction and Ekman pumping in the North Atlantic estimated by Marshall et al. (1993). It could be argued however that this vertical motion when averaged in the along-stream direction does not lead to a mean downwelling since opposing vertical circulations on opposite sides of a meander crest/trough cancel. The analysis of the observations suggests that while opposing vertical circulations were found on either side of a meander trough, the Lagrangian mean vertical velocity near the location of the intrusion was non-zero. This was because in transiting the two sides of the trough, the intrusion was observed to move towards the center of the Stream between the downwelling branches of the opposing vertical circulations, resulting in a downward Lagrangian mean vertical velocity and net subduction.

The inference of the Lagrangian mean vertical velocity was made possible by the combined use of the Eulerian omega-equation diagnostic and a Lagrangian analysis of the intrusion displacement, the latter of which could be performed since the observations were measured in a quasi-Lagrangian frame following a floating spar buoy drifting in the Stream. This makes this observational study on frontal vertical circulation unique relative to others described in the literature whose diagnostics are based primarily on solutions to the omega equation (e.g. Pollard and Regier 1992; Rudnick 1996; Naveira Garabato et al. 2001). In addition to revealing information on the Lagrangian mean vertical velocity, the combined Eulerian-Lagrangian analysis provides a means to test the representativeness of the solution of the omega equation to the observed vertical motions. This comparison has shown that the strain field associated with the Gulf Stream that forces the omega-equation (as opposed to winds,

diabatic processes, etc.) was the dominant driver of subduction at the front.

At an eddying front subduction is associated with both the along-front averaged cross-stream circulation as well as a bolus velocity that arises from correlations between the eddy velocity and isopycnal thickness perturbations (Marshall 1997). The downwelled intrusions and pycnostads were characterized by relatively thick isopycnal layer thicknesses. Hence the observations point to a correlation between downwelling and enhanced isopycnal thickness which would imply that there was a downward bolus velocity and a net subduction at the front. For flows with low Rossby and Burger numbers, the bolus velocity is proportional to minus the eddy flux of PV. Thus a downward bolus velocity corresponds to an upward eddy PV flux which is down the mean PV gradient at the locations of the intrusion and pycnostad. Hence the observations evidence the action of eddies to homogenize PV along isopycnals, consistent with the finite amplitude behavior of baroclinic instability (Marshall et al. 1999).

The bolus velocity associated with baroclinic instability can be expressed in terms of an eddy induced streamfunction that is thermally direct, i.e. in the sense to flatten isopycnals and release available potential energy. While the limited number of cross-stream sections made at the Gulf Stream do not permit the direct calculation of the eddy induced streamfunction, comparison of the strength of the thermally direct and indirect circulations upstream and downstream of the sampled meander trough suggests that the thermally direct circulation dominates, consistent with the energetics of baroclinic instability. A similar dominance of the thermally direct circulation was observed at the Antarctic Polar Front (Naveira Garabato et al. 2001) and the Azores Front (Rudnick 1996), pointing to the importance of baroclinic instability in driving frontolysis, restratification, and net subduction

at ocean fronts.

The thermohaline intrusion descended along the 26.3 kg m^{-3} isopycnal surface, which is in the seasonal pycnocline that capped the EDW at this early stage in the winter season. The pycnostad to the south of the Gulf Stream's center was found on the 26.15 kg m^{-3} isopycnal surface that resides beneath the stratified base of the warm core. The low PV water in these subducted features could have been formed by surface cooling or by winds directed along the frontal jet, the latter of which leads to Ekman advection of denser water over light, convective mixing, and a reduction of the stratification and PV (Thomas 2005). High-resolution frontal simulations suggest that subduction and transport of low PV surface waters on the submesoscale can contribute to the erosion of a pycnocline through an along isopycnal flux of PV (Thomas 2008). The subduction of the low PV intrusion and pycnostad described here may in an analogous manner contribute to the reduction of the stratification in the seasonal pycnocline and precondition both EDW for ventilation and the warm core for convective erosion. CLIMODE observations conducted in the winter of 2007 revealed that further downstream from the location of hydrographic survey described here, the Gulf Stream's warm core was absent, apparently having been eroded, and in its place was a frontal zone with regions of negative PV yet stable stratification evidencing symmetric and inertial instabilities (Joyce et al. 2009).

The formation of the thermohaline intrusion observed in the Gulf Stream is an example of how mesoscale motions can transfer salinity variance from the large scale to the submesoscale via along-isopycnal advection. Smith and Ferrari (2009) have shown that such submesoscale compensated thermohaline variance can be efficiently dissipated by vertical mixing processes when these submesoscale features are associated with a vertically-sheared flow. It is possible

that by this mechanism thermohaline intrusions formed by meanders in the vertically-sheared Gulf Stream could play an important role in mixing the large-scale cross-gyre salinity gradient that delineates the front. Studying the dynamics of this process will be the subject of future research.

Acknowledgments.

We wish to thank all of our colleagues in CLIMODE for their efforts to study this interesting region, and collect an excellent data set for us to examine here. Of particular help was the ODF group at Scripps for their CTD efforts, the remote SST and SSH group at UW for their daily images which guided our seagoing work and assisted in this analysis, Frank Bahr and Barry Walden at WHOI for their efforts to install and set up the shipboard ADCP, and Captain Silva and the crew of the Atlantis who experienced an abrupt climate change from their usual fairweather cruises to the East Pacific Rise. The work was part of CLIMODE (www.climode.org), a process study of US CLIVAR. Support came from the National Science Foundation grant OCE-0424865 [TJ & LT]. LT was also supported by NSF grant OCE-0549699 and the Worzel Assistant Scientist Endowed Fund at WHOI.

REFERENCES

- Allen, J. T. and D. A. Smeed, 1996: Potential vorticity and vertical velocity at the Iceland-Faeroes front. *J. Phys. Oceanogr.*, **26**, 2611–2634.
- Andrews, D., J. Holton, and C. Leovy, 1987: *Middle Atmosphere Dynamics*, chap. 3, 133–137. Academic Press.
- Bower, A. S. and T. Rossby, 1989: Evidence of cross-frontal exchange processes in the Gulf Stream based on isopycnal RAFOS float data. *J. Phys. Oceanogr.*, **19**, 1177–1190.
- Giordani, H., L. Prieur, and G. Caniaux, 2006: Advanced insights into sources of vertical velocity in the ocean. *Ocean Dynamics*, **56**, 513–524.
- Hoskins, B. J., I. Draghici, and H. C. Davies, 1978: A new look at the ω -equation. *Qt. J. R. Met. Soc.*, **104**, 31–38.
- Huang, R. X. and B. Qiu, 1994: Three-dimensional structure of the wind-driven circulation in the subtropical gyre of the North Pacific. *J. Phys. Oceanogr.*, **24**, 1608–1622.
- Joyce, T. M., L. N. Thomas, and F. Bahr, 2009: Wintertime observations of Subtropical Mode Water formation within the Gulf Stream. *Geophys. Res. Lett.*, **36**, L02607, doi:10.1029/2008GL035918.
- Lindstrom, S. S., X. Qian, and D. R. Watts, 1997: Vertical motion in the Gulf Stream and its relation to meanders. *J. Geophys. Res.*, **102**, 8485–8503.

- Marshall, D., 1997: Subduction of water masses in an eddying ocean. *J. Mar. Res.*, **55**, 201–222.
- Marshall, D. P., R. G. Williams, and M. M. Lee, 1999: On the relation between eddy-induced transport and the isopycnic gradients of potential vorticity. *J. Phys. Oceanogr.*, **29**, 1571–1578.
- Marshall, J. C., A. J. G. Nurser, and R. G. Williams, 1993: Inferring the subduction rate and period over the North Atlantic. *J. Phys. Oceanogr.*, **23**, 1315–1329.
- Nagai, T., A. Tandon, and D. L. Rudnick, 2006: Two-dimensional ageostrophic secondary circulation at ocean fronts due to vertical mixing and large-scale deformation. *J. Geophys. Res.*, **111**, C09038, doi:10.1029/2005JC002964.
- Naveira Garabato, A. C., J. T. Allen, H. Leach, V. H. Strass, and R. T. Pollard, 2001: Mesoscale subduction at the Antarctic Polar Front driven by baroclinic instability. *J. Phys. Oceanogr.*, **31**, 2087–2107.
- Niiler, P., 1969: On the Ekman divergence in an oceanic jet. *J. Geophys. Res.*, **74**, 7048–7052.
- Pollard, R. T. and L. A. Regier, 1992: Vorticity and vertical circulation at an ocean front. *J. Phys. Oceanogr.*, **22**, 609–625.
- Rudnick, D. L., 1996: Intensive surveys of the Azores Front. 2. Inferring the geostrophic and vertical velocity fields. *J. Geophys. Res.*, **101 (C7)**, 16 291–16 303.
- Smith, K. S. and R. Ferrari, 2009: Production and dissipation of compensated t-s variance by mesoscale stirring in the NATRE region. *J. Phys. Oceanogr.*, in press.

- Spall, M. A., 1995: Frontogenesis, subduction, and cross-front exchange at upper ocean fronts. *J. Geophys. Res.*, **100**, 2543–2557.
- Stern, M. E., 1965: Interaction of a uniform wind stress with a geostrophic vortex. *Deep-Sea Res.*, **12**, 355–367.
- The CLIMODE Group, 2008: Climode: a mode water dynamics experiment in support of CLIVAR. *Bull. Amer. Meteor. Soc.*, submitted.
- Thomas, L. N., 2005: Destruction of potential vorticity by winds. *J. Phys. Oceanogr.*, **35**, 2457–2466.
- Thomas, L. N., 2008: Formation of intrathermocline eddies at ocean fronts by wind-driven destruction of potential vorticity. *Dyn. Atmos. Oceans*, **45**, 252–273, doi:10.1016/j.dynatmoce.2008.02.002.
- Thomas, L. N., C. M. Lee, and Y. Yoshikawa, 2009: The subpolar front of the Japan/East Sea II: Inverse method for determining the frontal vertical circulation. *J. Phys. Oceanogr.*, submitted.
- Viúdez, A., J. Tintoré, and R. L. Haney, 1996: About the nature of the generalized omega equation. *J. Atmos. Sci.*, **53**, 787–795.
- Worthington, L. V., 1959: The 18° water in the Sargasso Sea. *Deep-Sea Res.*, **5**, 297–305.
- Worthington, L. V., 1976: *On the North Atlantic Circulation*. The John Hopkins University Press, 110 pp.

List of Figures

- 1 The SST (contours) on January 24, 2006 and the locations of the hydrographic stations (dots) occupied during the cruise. Stations where a thermohaline intrusion was observed (i.e. 22, 31, and 41 on lines 2, 3, and 4, respectively) are denoted with stars. Stations where a pycnostad was observed on the southern edge of the Gulf Stream (i.e. 18 and 28 on lines 2 and 3, respectively) are denoted with diamonds. The contour interval for the SST is 1 °C. The thick gray line marks the trajectory of the spar buoy. The arrows indicate the direction of the cross-stream, x_s , and along-stream, y_s , coordinates. 24
- 2 Cross-stream sections along line 3 of the salinity, apparent oxygen utilization, down-stream velocity, planetary potential vorticity and potential density (contours). The locations of the hydrographic stations are indicated at the top of each panel. The contour interval for the density is 0.2 kg m⁻³. Note that the colorscale for the PV does not reflect its full range of values, and was chosen to highlight regions with low PV. The maximum value of the PV on this section was 2.1×10^{-8} s⁻³. In the panel of the down-stream velocity, the isotach corresponding to the depth-averaged velocity at the location of the spar buoy (which was coincident with station 29 on the section) is indicated in gray. Note that the cross-stream coordinate x_s increases moving from the dense to less dense side of the main front of the Gulf Stream. 25

3	Hydrographic evidence of subduction of a thermohaline intrusion in the northern wall of the Gulf Stream. Profiles of the salinity (left), apparent oxygen utilization (right), and potential density (middle) taken at stations 22 (dark gray), 31 (thin black), and 41 (light gray) where the intrusion was observed (see Figure 1 for the positions of these stations). In the inset, the temperature-salinity relation at these stations is plotted along with the potential density (dashed contours of interval 0.5 kg m^{-3}).	26
4	The lagged correlation between salinity profiles from stations 22 and 31 (solid black), 31 and 41 (dashed), and 18 and 28 (solid gray). The lag corresponds to the downward shift of the previous cast to the subsequent cast. The correlations were calculated using data collected in the depth range of $z > -550$ m for casts 22,31, and 41 and $z > -350$ m for casts 18 and 28.	27
5	The observed cross-stream velocity along line 2 (left) and line 4 (right). The potential density is shown as well (thin contours) at an interval of 0.2 kg m^{-3} . Note that a positive cross-stream velocity, $u_s > 0$, corresponds to flow moving from the dense to less dense side of the main front of the Gulf Stream. . . .	28
6	The inferred vertical velocity along line 2 (left) and line 4 (right). Thick black, gray, and dashed contours denote negative, positive, and zero values for the vertical velocity. The contour interval for w is 10 m day^{-1} . The potential density is shown as well (thin contours) at an interval of 0.2 kg m^{-3}	29

7 Hydrographic evidence of subduction of a pycnostad near the southern edge of the Gulf Stream's warm core. Profiles of the salinity (left), apparent oxygen utilization (right), and potential density (middle) taken at stations 18 (gray) and 28 (black). See Figure 1 for the positions of these stations. In the inset, the temperature-salinity relation at these stations is plotted along with the potential density (dashed contours of interval 0.5 kg m^{-3}). 30

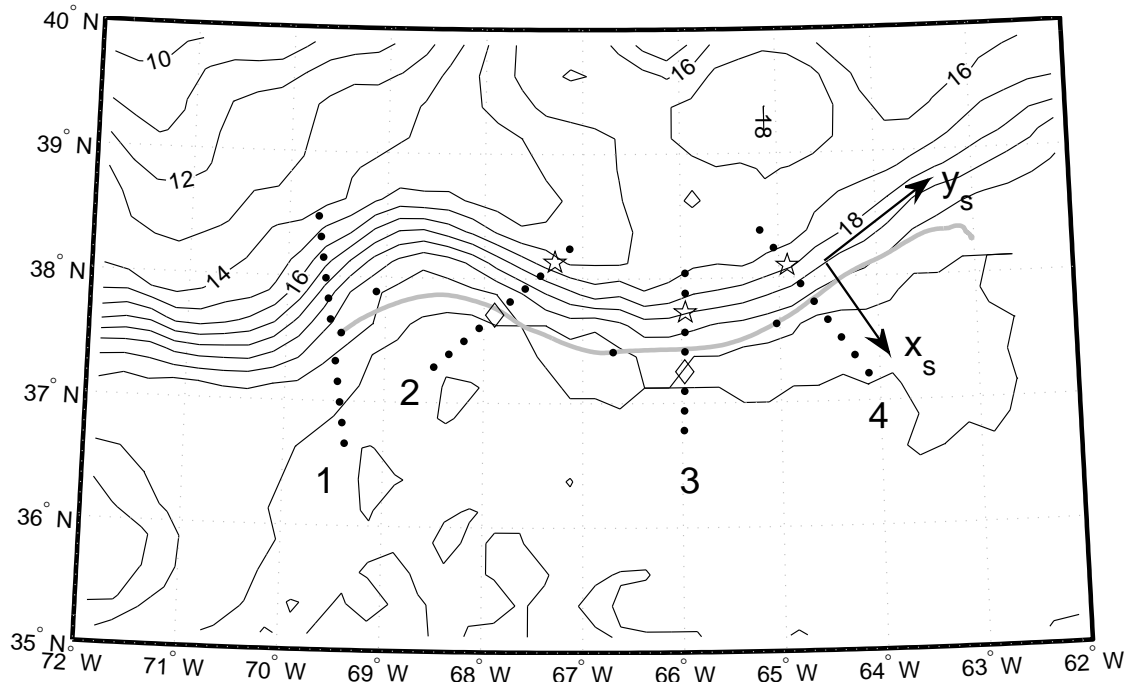


FIG. 1. The SST (contours) on January 24, 2006 and the locations of the hydrographic stations (dots) occupied during the cruise. Stations where a thermohaline intrusion was observed (i.e. 22, 31, and 41 on lines 2, 3, and 4, respectively) are denoted with stars. Stations where a pycnostad was observed on the southern edge of the Gulf Stream (i.e. 18 and 28 on lines 2 and 3, respectively) are denoted with diamonds. The contour interval for the SST is $1\text{ }^{\circ}\text{C}$. The thick gray line marks the trajectory of the spar buoy. The arrows indicate the direction of the cross-stream, x_s , and along-stream, y_s , coordinates.

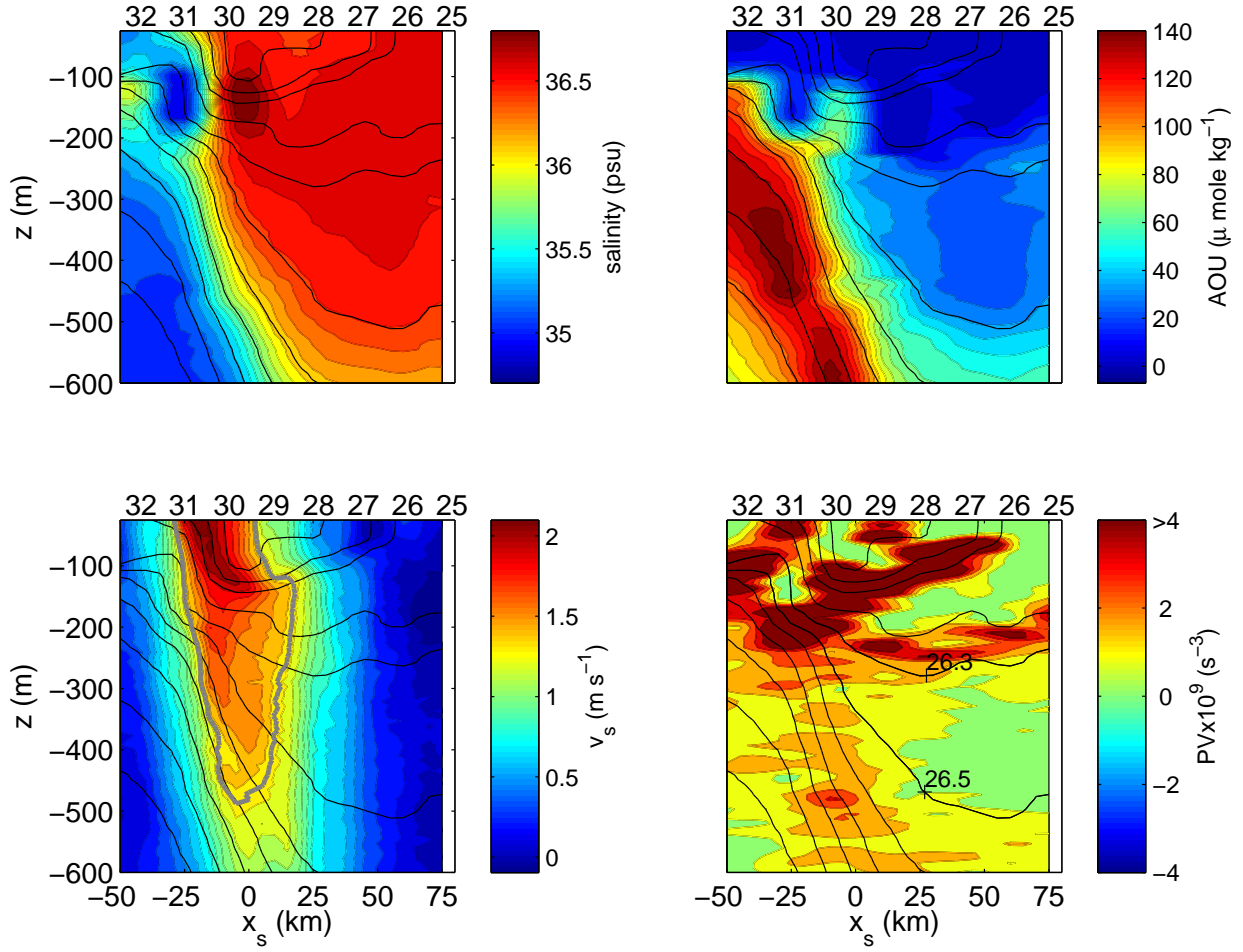


FIG. 2. Cross-stream sections along line 3 of the salinity, apparent oxygen utilization, downstream velocity, planetary potential vorticity and potential density (contours). The locations of the hydrographic stations are indicated at the top of each panel. The contour interval for the density is 0.2 kg m^{-3} . Note that the colorscale for the PV does not reflect its full range of values, and was chosen to highlight regions with low PV. The maximum value of the PV on this section was $2.1 \times 10^{-8} \text{ s}^{-3}$. In the panel of the down-stream velocity, the isotach corresponding to the depth-averaged velocity at the location of the spar buoy (which was coincident with station 29 on the section) is indicated in gray. Note that the cross-stream coordinate x_s increases moving from the dense to less dense side of the main front of the Gulf Stream.

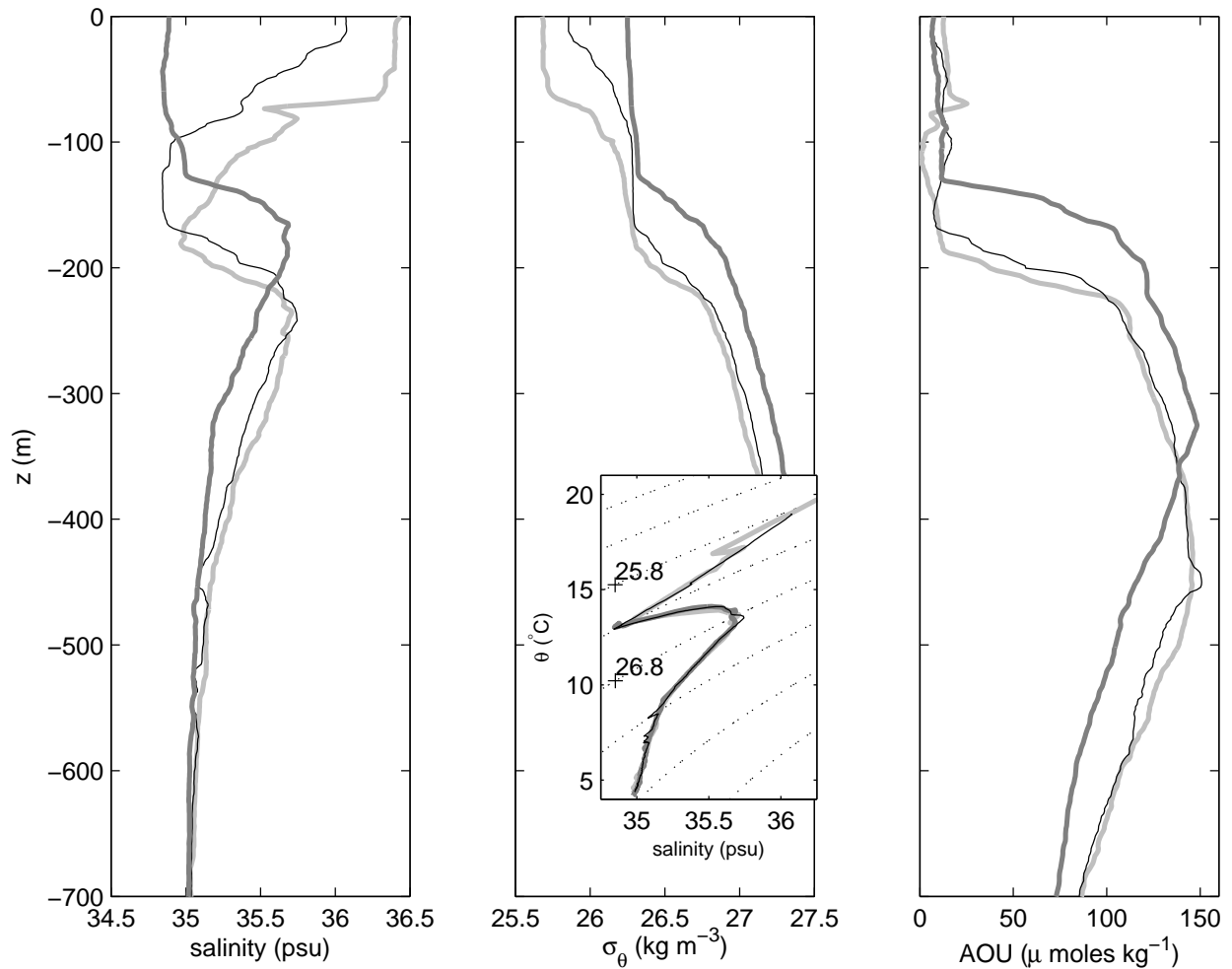


FIG. 3. Hydrographic evidence of subduction of a thermohaline intrusion in the northern wall of the Gulf Stream. Profiles of the salinity (left), apparent oxygen utilization (right), and potential density (middle) taken at stations 22 (dark gray), 31 (thin black), and 41 (light gray) where the intrusion was observed (see Figure 1 for the positions of these stations). In the inset, the temperature-salinity relation at these stations is plotted along with the potential density (dashed contours of interval 0.5 kg m^{-3}).

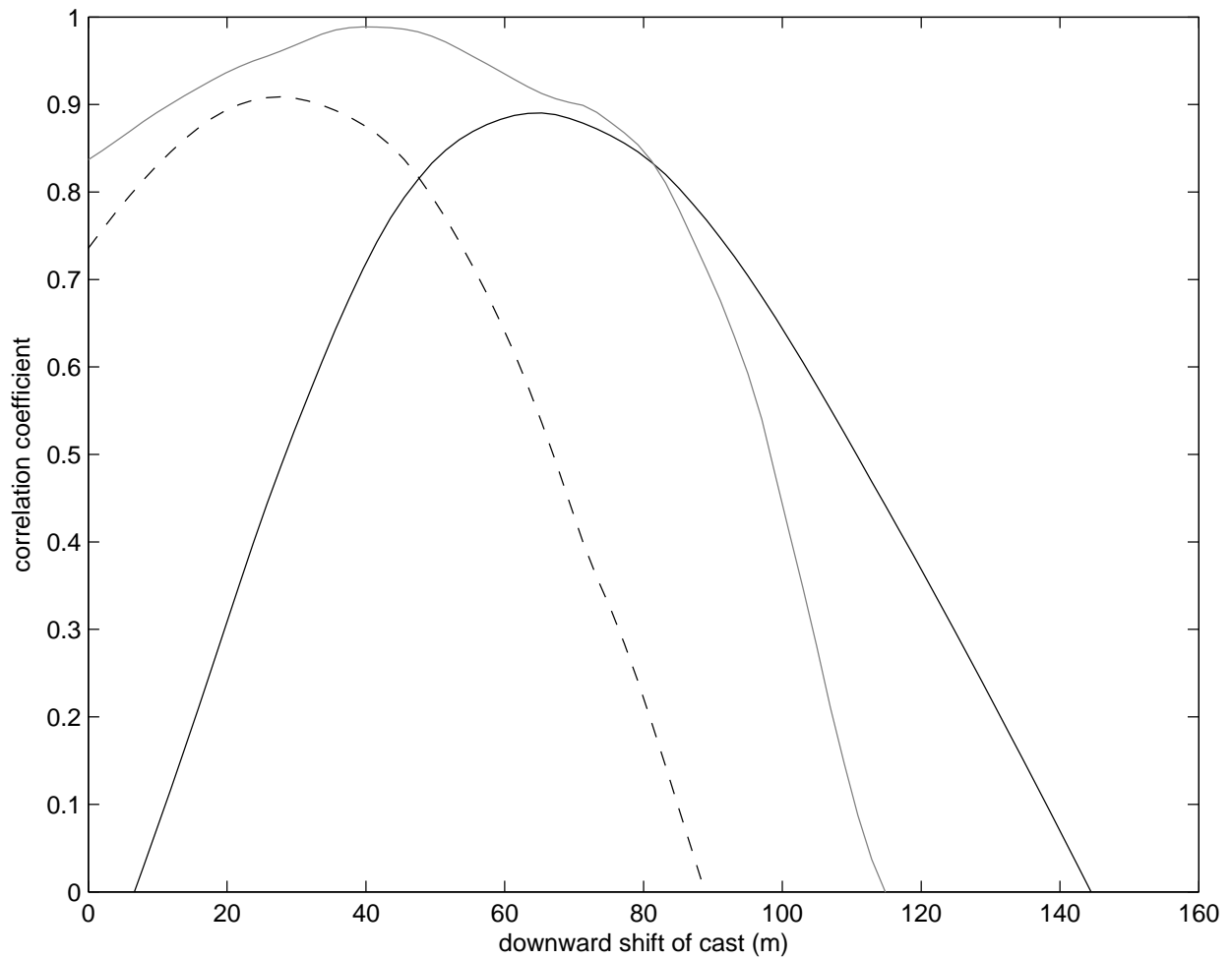


FIG. 4. The lagged correlation between salinity profiles from stations 22 and 31 (solid black), 31 and 41 (dashed), and 18 and 28 (solid gray). The lag corresponds to the downward shift of the previous cast to the subsequent cast. The correlations were calculated using data collected in the depth range of $z > -550$ m for casts 22,31, and 41 and $z > -350$ m for casts 18 and 28.

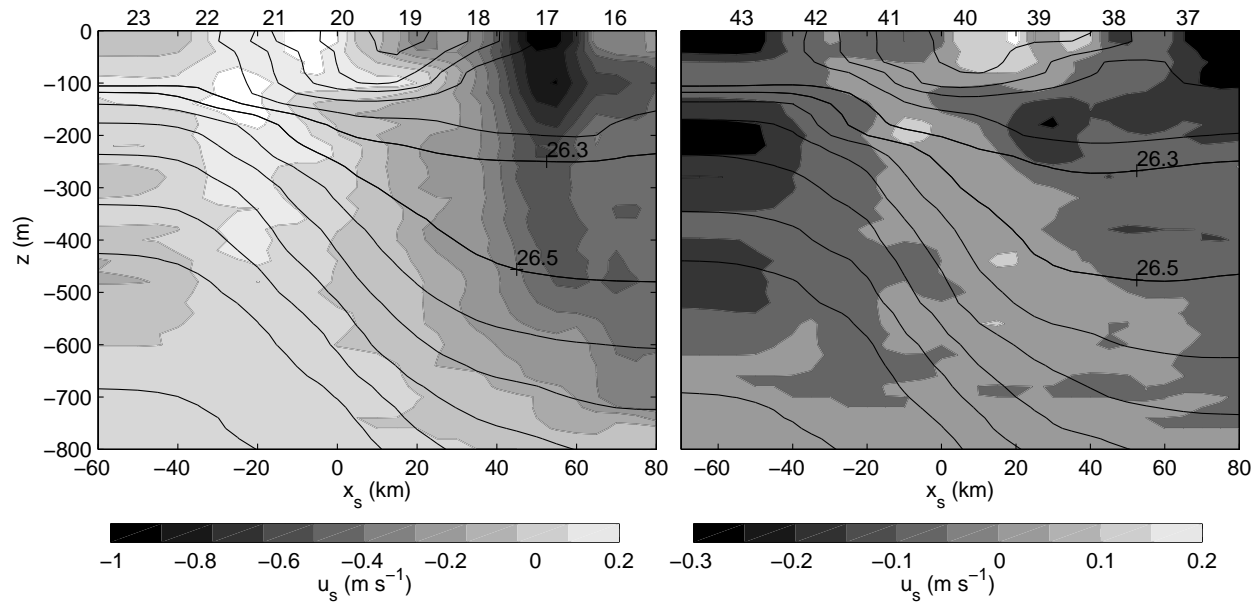


FIG. 5. The observed cross-stream velocity along line 2 (left) and line 4 (right). The potential density is shown as well (thin contours) at an interval of 0.2 kg m^{-3} . Note that a positive cross-stream velocity, $u_s > 0$, corresponds to flow moving from the dense to less dense side of the main front of the Gulf Stream.

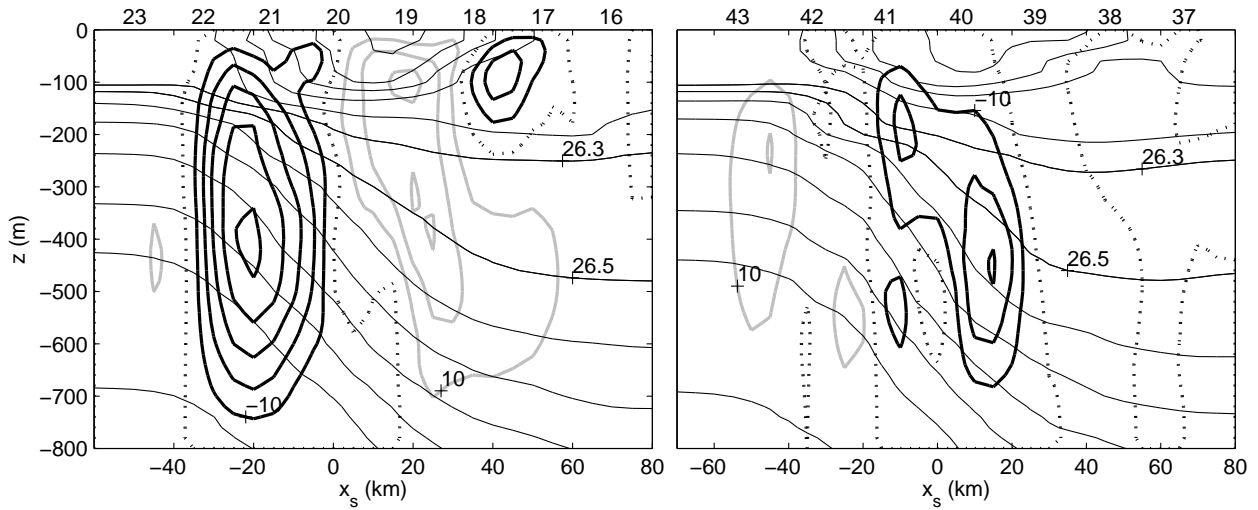


FIG. 6. The inferred vertical velocity along line 2 (left) and line 4 (right). Thick black, gray, and dashed contours denote negative, positive, and zero values for the vertical velocity. The contour interval for w is 10 m day^{-1} . The potential density is shown as well (thin contours) at an interval of 0.2 kg m^{-3} .

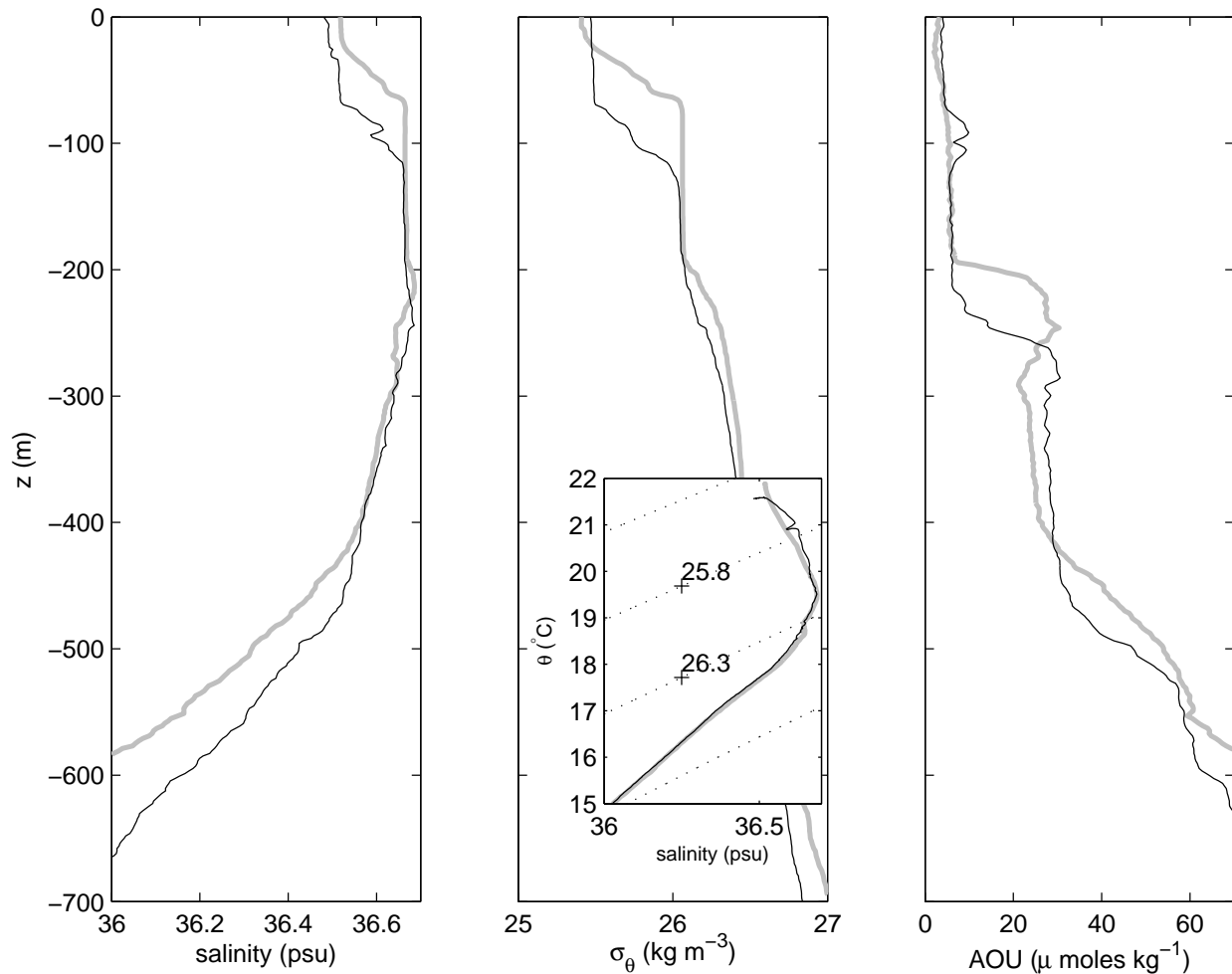


FIG. 7. Hydrographic evidence of subduction of a pycnostad near the southern edge of the Gulf Stream’s warm core. Profiles of the salinity (left), apparent oxygen utilization (right), and potential density (middle) taken at stations 18 (gray) and 28 (black). See Figure 1 for the positions of these stations. In the inset, the temperature-salinity relation at these stations is plotted along with the potential density (dashed contours of interval 0.5 kg m^{-3}).